Catalysis Today 170 (2011) 110–119

Contents lists available at ScienceDirect

Catalysis Today

journal homepage: www.elsevier.com/locate/cattod

Mass transport effects in the borohydride oxidation reaction—Influence of the residence time on the reaction onset and faradaic efficiency

Kênia S. Freitas[a,b], Belen Molina Concha[a], Edson A. Ticianelli[b], Marian Chatenet[a,*]

[a] Laboratoire d'Electrochimie et de Physicochimie des Matériaux et des Interfaces, LEPMI, UMR 5279 CNRS/Grenoble-INP/Université de Savoie/Université Joseph Fourier, BP 75, 38402 Saint-Martin d'Hères Cedex, France

[b] Instituto de Química de São Carlos, Universidade de São Paulo, Av. Trab. São-carlense 400, CP 780, CEP 13560-970 São Carlos, SP, Brazil

ARTICLE INFO

Article history:
Received 27 October 2010
Received in revised form 5 January 2011
Accepted 27 January 2011
Available online 8 March 2011

Keywords:
Borohydride oxidation reaction (BOR)
Gold
Platinum
Residence time
Faradaic efficiency
Reaction onset

ABSTRACT

The borohydride oxidation reaction (BOR) was studied on Pt and Au electrodes by cyclic voltammetry in dilute alkaline borohydride solutions (0.1 M NaOH + 10^{-3} mol L^{-1} $NaBH_4$). More specifically, the electrodes were considered as either Vulcan XC72-supported Pt or Au (noted as Pt/C and Au/C, respectively) active layers or smooth Pt or Au surfaces, the latter possibly being covered by a layer of (non-metalized) Vulcan XC72 carbon powder. The BOR onset potential and the number of electrons (n_{e^-}) exchanged per BH_4^- anion (faradaic efficiency) were investigated for these electrodes, to determine whether the residence time of reaction intermediates (at the electrode surface or inside the porous layer) does influence the overall reaction pathway/completion. For the carbon-supported platinum, n_{e^-} strongly depends on the thickness of the active layer. While thin (ca. 0.5 μm-thick) Pt/C active layers yield $n_{e^-} < 4$, thick layers (approximately 3 μm) yield $n_{e^-} \approx 8$, which can be ascribed to the sufficient residence time of the molecules formed within the active layer (H_2, by heterogeneous hydrolysis, or BOR intermediates) enabling further (near-complete) oxidation. This puts into evidence that not only the nature of the electrocatalyst is important to reach high BOR efficiency, but also the structure/thickness of the active layer. The same trend applies for Au/C active layers and for smooth Pt or Au surfaces covered with a layer of (inactive) Vulcan XC72. In addition, the BOR onset usually shifts negative when the reaction intermediates are trapped, which suggests that some of the intermediates are more easily oxidized than BH_4^- itself; based on literature data, BH_3OH^- species is a likely candidate.

1. Introduction

Despite intense research efforts since a decade [1–8], the direct borohydride fuel cell (DBFC) is still not widely available as a generator for portable electronic devices. Among other hindrances, the DBFC remains limited by its complex anodic reaction, the borohydride oxidation reaction (BOR). The BOR involves 8 electrons and 8 hydroxyl anions per BH_4^- species (Eq. (1)).

$$BH_4^- + 8OH^- \rightarrow BO_2^- + 6H_2O + 8e^- \quad (E^0 = -1.24V \text{ vs. SHE}) \quad (1)$$

While such high (theoretical) electron count per BH_4^- anion coupled with the low (theoretical) electrode potential is advantageous from an energy density prospect, it also consists of a drawback, because the reaction must obviously occur in multiple steps, some of which possibly being slow. In addition, whereas the homogeneous hydrolysis of BH_4^- is virtually suppressed for electrolytic solutions of high pH [9], the heterogeneous hydrolysis of the tetrahydroborate anion is at stake on a variety of electrode materials. Like the BOR, the heterogeneous hydrolysis of BH_4^- is a sequential multi-steps reaction [10], often described by Eqs. (2) and (3).

$$BH_4^- + H_2O \rightarrow BH_3OH^- + H_2 \quad (2)$$

$$BH_3OH^- + H_2O \rightarrow BO_2^- + 3H_2 \quad (3)$$

The competition between the heterogeneous hydrolysis and the direct oxidation of BH_4^- eventually undergo the occurrence of numerous electrochemical (E) or chemical (C) steps, yielding numerous boron-intermediate species [11,12]. While the seek for these intermediate BOR products was rendered complex and formerly somewhat speculative [11,13–15], because of both the complexity of the boron chemistry in aqueous media [12] and the lack of *in situ* physical techniques, recent papers have now unveiled some of the uncertainties on that point. In particular, the nature of some BOR intermediates has been discovered for gold electrodes [16–19]: they can consist of partly de-hydrided borohydride species (e.g. BH_3 or BH_2-based species, as detected by *in situ* Fourier transformed infra red (FTIR) spectroscopy [16,17]),

* Corresponding author. Tel.: +33 476826588; fax: +33 476826777.
E-mail address: Marian.Chatenet@grenoble-inp.fr (M. Chatenet).

0920-5861/$ – see front matter © 2011 Elsevier B.V. All rights reserved.
doi:10.1016/j.cattod.2011.01.051

and molecular hydrogen (H_2), as detected by volumetric analyses [5,20,21] or on-line electrochemical mass spectrometry (OLEMS) [19,22]. It is obvious that the generation of H_2, a very diffusive gas, can yield to H_2 losses, further resulting in lower faradaic efficiency, even when the anode electrocatalyst is capable of ionizing hydrogen (e.g. Pt). Should H_2 be formed on anode materials not capable of valorizing H_2 (e.g. Au or Ag), this would result in larger faradaic losses. As an illustration, the BOR faradaic efficiency on Au remains strictly lower than 100% in the low potential region ($E < 0.6$ V vs. RHE), where strong hydrogen evolution is monitored in OLEMS [19,22], as confirmed by several other recent papers [18,19,23,24].

Concerning the partly de-hydrided borohydride species mentioned above, the recent findings from Molina Concha et al. obtained during the BOR on smooth gold surfaces pointed towards the existence of BH_2 or BH_3 species either adsorbed (further enabling the reaction completion) or in solution (Fig. 1) [16]. Whereas the band intensities (proportional to the amount of species present in the volume of solution probed) for the species at the electrode surface (Fig. 1A and B) reach a maximum upon potential increase, the total amount of these species in the thin-film of solution monotonously increases with the potential (Fig. 1C). The latter observation is compatible with a continuous production of BH_2 and BH_3 species at the electrode surface that quickly desorb and diffuse into the solution. It is wise noting that, unlike H_2 that is unambiguously produced by hydrolysis (Eqs. (2) and (3)), such BH_2 or BH_3 intermediates are likely generated in the course of the direct BOR pathway. So, suppressing the hydrolysis of BH_4^-, should it be possible, would therefore not be sufficient to guarantee complete faradaic efficiency during the BOR; losses in BOR intermediate species by their back-diffusion away from the electrode surface would also lower the BOR faradaic efficiency.

Moving back to this well known (in the case of H_2) concept of "back-diffusion" of reaction intermediates away from the electrode surface, it did yield to a few interesting studies concerning the importance of the electrode structure on the BOR faradaic efficiency [25–29]. Indeed, the geometry/structure of the electrode rules the mass-transport of reactant, intermediates and (by)products at/within the electrode. In that frame, Liu et al. found that the hydrogen evolution occurring at their porous nickel anode (resulting from significant BH_4^- hydrolysis) influenced the cell performance, by generating bubbles that could accumulate in the anode and at the anode|membrane interface, thereby decreasing the contact area of the fuel with the electrode and blocking the ion transport to the membrane [29]. As a possible solution, they proposed anodes of increased porosity and non-zero gap cells [29]. In the same line, Cheng and Scott demonstrated the interest of using a Ti-mesh electrode substrate instead of the classical bounded carbon-supported anodes, the rationale for this being the very open structure of the mesh, enabling better borohydride mass-transport and faster (H_2) gas bubble release [28]. These authors further studied the influence of the flow field geometry and flow rate for the tetrahydroborate feeding of a DBFC, but concluded that their effects were small [30]. This likely results from the BOR overall sluggishness [23,31–36]: there is more to gain in valorizing all the intermediates generated by the BOR/BH_4^- hydrolysis, than to supply large amounts of BH_4^-. Indeed increasing the BH_4^- flux to the anode would likely (i) yield faster homogeneous/heterogeneous hydrolysis [1,10] and (ii) not result in quantitative oxidation, as a result of the slow BOR kinetic (rotating disk electrode (RDE) experiments performed in concentrated solutions demonstrated very well that, above ca. 0.1 M $NaBH_4$, the expected diffusion-convection plateau is not reached for BOR overvoltage as large as 1 V on Pt/C [37] and 2 V on Au [31].

This short selected literature review demonstrates how difficult it is to determine the actual effectiveness of an electrocatalyst material to perform the direct (electrochemical) BOR, as formerly pointed out by Morris et al. back in the 1980s [12]: "This system is complicated by the presence of a competitive chemical reaction (hydrolysis) that gives products that are themselves oxidizable at somewhat more negative potentials than the parent ion. A further complication is introduced by the pH dependence of the rate of formation of these hydrolysis products (i.e. BH_3OH^-, $BH_2OH_2^-$, $BHOH_3^-$). As a final complication, the composition of the elec-

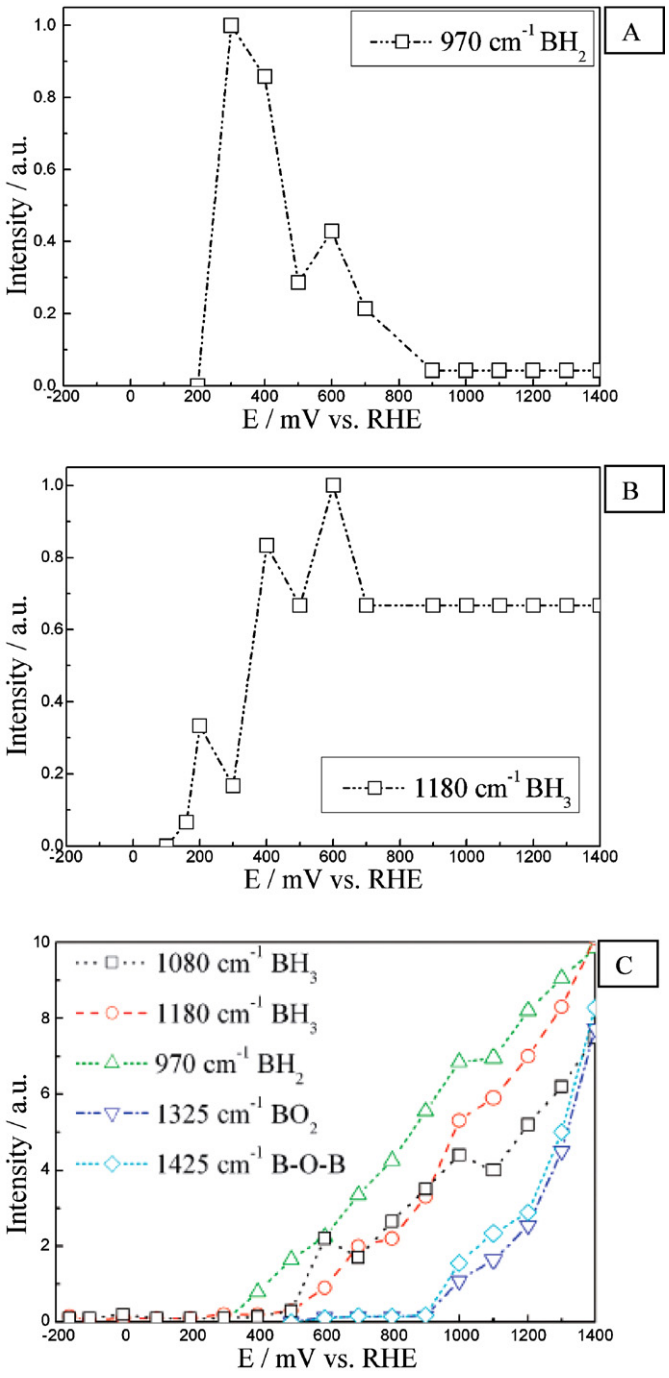

Fig. 1. Evolution of the FTIR band intensities in p-polarized light (p-polarized light is essentially sensitive to the species at the electrode surface) for (A) BH_2 and (B) BH_3 bands or (C) non-polarized light (in non-polarized light, all the solution in the thin-film between the Au electrode and the ZnSe flat window is probed (i.e. species at the electrode surface and in solution)) during the BOR on Au electrode in 1 M NaOH + 1 M $NaBH_4$ solution ($T = 25\,^\circ C$).
Reproduced from Ref. [16], with permission of the Royal Society of Chemistry.

trode surface, by virtue of its role as heterogeneous catalyst for the hydrolysis reaction, also influences the overall composition of a tetrahydroborate analyte . . .". The case of platinum, one of the most studied DBFC anode materials, further illustrates this issue: the BOR mechanism on platinum remains uncertain [10–12,23,26,38] and no consensus exists, whether Pt yields to low or high faradaic efficiency. The number of electron exchanged per BH_4^- anion, n_{e-}, was indeed reported to vary from 2 to ca. 8 on Pt [23,26,27,37–41], with very different trends observed: strong heterogeneous hydrolysis [5,37,38,40,41] versus moderate heterogeneous hydrolysis [23,27]. Such apparent variable completion of the BOR can be related to true kinetic effects or/and to mass-transport effects at (within) the Pt (Pt/C) electrode (the latter depending also on the experimental setup/conditions used to characterize the BOR). Actually, a clear distinction should be made between the behavior of Pt in open-circuit potential (ocp) and upon polarization. In the former case (ocp), platinum strongly evolves hydrogen; this apparent drawback has nevertheless been positively addressed by using Pt as an H_2-evolution catalyst to *in situ* supply a fuel cell with pure H_2 [42]. In the latter case, it seems that the heterogeneous hydrolysis of BH_4^- can be either slowed down [23] or that the reaction products can be near-completely utilized when the potential is positive to the ocp [27]. In particular, the recent findings from Molina Concha and Chatenet did point towards the importance of mass-transport on the faradaic efficiency on Pt/C electrodes, near-complete faradaic efficiency being reached for adequate Pt/C active layer structure [27]. This example shows that the apparent faradaic efficiency of one BOR electrocatalyst is likely to depend, not only on the nature of the electrode material, but also on the geometry of the electrode/active layer considered. This issue is of extreme importance, because it could affect the greatest advantage of the DBFC, namely the high energy density of its fuel. It is wise pointing out that the importance of mass-transport issues in the overall completion of a multi-step reaction pathway has already been put into evidence for other reactions of electrocatalytic interest, like the oxygen reduction reaction (ORR) [43–47] or the methanol oxidation reaction [48,49]. For example, it is now well admitted that the ORR would proceed by a sequential 2-electron reaction (yielding H_2O_2) followed by H_2O_2 electroreduction/decomposition at the electrode surface (or within the electrode active layer), resulting in an overall 4-electron pathway, when the H_2O_2 intermediate species cannot escape from the active sites/active layers [47]. In other words, the apparent number of electrons exchanged per O_2 molecule can substantially deviate from 4 (by inferior values) when the amount of active sites decrease, thereby favoring the escape of H_2O_2 back to solution.

In that frame, the present paper aims at complementing the data obtained so far on the topic, by systematically focusing on the mass-transport effects in the course of the BOR. The electrode materials studied are based on the two most classical BOR electrocatalyst of the literature, namely platinum and gold. In both cases, smooth polycrystalline electrodes and Vulcan XC72-supported active layers of various thicknesses are investigated to evidence possible mass-transport/residence time effects on the number of electrons involved in the BOR (faradaic efficiency). Finally, as some of the intermediates generated in the course of the heterogeneous hydrolysis/direct oxidation of BH_4^- are oxidized at a lower potential than BH_4^- itself [12] (e.g. BH_3OH^- [15,18,50,51]), the BOR onset potential is also surveyed in view of the morphology of the Pt or Au-based electrode.

2. Experimental procedures

The smooth polycrystalline Pt and Au electrodes were polished using diamond paste down to 1 μm, followed by subsequent washing for 15 min in successive ultrasonic baths of acetone, ethanol and water, in order to remove any trace of impurities.

The carbon-supported samples (Au/C and Pt/C, C = Vulcan XC72, in all cases from E-Tek Inc.) samples were investigated in catalytic active layers deposited on a glassy carbon electrode (diameter 5 mm). Like for the smooth metal electrodes, the glassy carbon substrate was previously polished and cleaned prior to active layer deposition. The active layer precursor was an ink containing a mixture of catalyst powder (Pt/C or Au/C) and polytetrafluoroethylene (PTFE, from a latex suspension) in a water:ethanol solution (3:1 in volume). The PTFE composition was held at 10 wt.% of the overall dry weight. In some cases, the active layer consisted of a blend between Pt/C (10, 20 or 40 wt.% Pt) or Au/C (10 wt.% Au) and Vulcan XC72 carbon. After sonication for 1 h, 10 μL of the mixture was deposited onto the glassy carbon electrode. After the solvent evaporation at room temperature, the active layer was sintered for 15 min at 150 °C in order to obtain sufficient mechanical stability. Unless otherwise stated, the equivalent active layer thickness (hereafter simply noted as thickness) was varied in the sequence: 3, 1.5, 0.75 and 0.38 μm. In all case, the active layer thickness was calculated assuming the loading and density of the dry materials (carbon-supported electrocatalyst + PTFE) at the glassy carbon RDE tip, according to the procedure employed formerly in the laboratory [44,52–55].[1] The thinner active layers were obtained by simply depositing a 10 μL drop of diluted ink (two, four or eight times diluted) onto the glassy carbon disk. It is wise stating that in all case the Pt/C (or Au/C) active layer was completely covering the glassy carbon surface, as demonstrated by optical microscopy (not shown for brevity). Therefore, using the well-known Levich equation (Eq. (4)), the limiting current variations observed experimentally in the following sections can be ascribed to faradaic efficiency variations and not to geometric area variations.

$$i_L = 0.620 n_{e-} F D^{2/3} C^* \nu^{-1/6} \Omega^{1/2} \quad (4)$$

where i_L (A cm^{-2}) is the limiting current density, n_{e-} is the number of electrons involved in the reaction in the limiting current region, D (cm^2 s^{-1}) is BH_4^- diffusion coefficient [24], C^* (mol cm^{-3}) is the BH_4^- concentration in solution, ν (cm^2 s^{-1}) is the solution kinematic viscosity [24] and Ω (rad s^{-1}) is the RDE revolution rate. The authors acknowledge that n_{e-} may vary as a function of the electrode potential, as lately documented in the literature [19,23,31,32,34]. However, for the sake of simplicity, the "apparent" n_{e-} will only be investigated in the limiting current region in the present study.

In some cases, the smooth Pt or Au electrodes were also prepared as stated above, prior to deposition of a layer of inactive (non-metalized) Vulcan XC72 at its surface, the thickness of which was varying in the range 0.38–3 μm (thicknesses calculated as explained above). Such inert deposit is labeled inert carbon layer (ICL) in the following.

The electrolytic solutions (0.1 M NaOH + 10^{-3} M $NaBH_4$ and 0.1 M NaOH + 10^{-3} M NH_3BH_3) were prepared using high purity sodium hydroxide, ammonia borane and sodium borohydride salts (Merck Suprapur®). The electrochemical experiments were conducted in a classical 3-electrode cell made of Pyrex® glass, after overnight cleaning in concentrated H_2SO_4–H_2O_2 mixture and thor-

[1] Let the authors precise that the important parameter to know is not the real thickness (t_{real}) of active layer (AL) but how this thickness varies from one electrode to the other. t_{real} varies like the equivalent thickness of Pt/C + PTFE (t_{eq}, i.e. the thickness of a non-porous Pt/C + PTFE layer) divided by $(1-\theta)$, with θ the pore volume fraction of the AL: $t_{real} = t_{eq}/(1-\theta)$. θ could not be measured due to the very small amount of material in each AL, but is nevertheless identical for all AL (implying: $1-\theta$ = constant), because the same carbon black material: Vulcan XC72, and the same [PTFE/Pt/C] ratio were used for all the AL studied. Therefore t_{real} scales linearly with t_{eq} and knowing t_{eq} is sufficient to compare several AL between them.

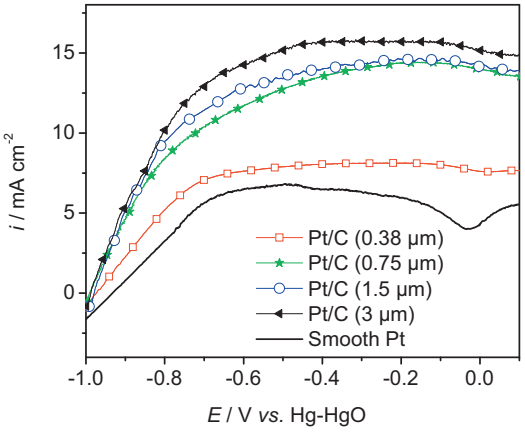

Fig. 2. $NaBH_4$ oxidation voltammograms in 0.1 M NaOH + 1 mM $NaBH_4$ (25 °C, argon atmosphere) plotted on Pt/C active layers of various thicknesses and on smooth Pt (Ω = 2500 rpm, ν = 5 mV s^{-1}).

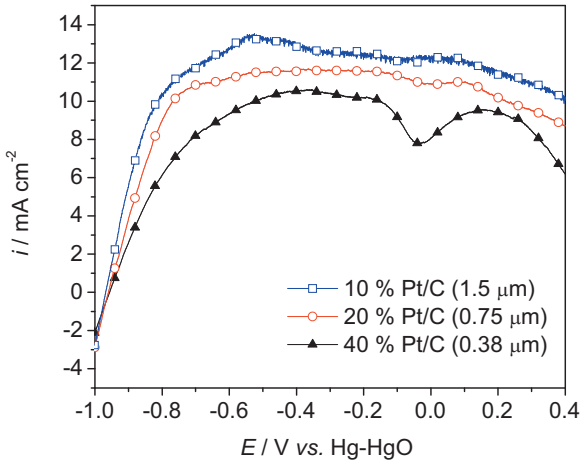

Fig. 3. $NaBH_4$ oxidation voltammograms plotted on Pt/C + Vulcan XC72 active layers of constant Pt-loading (m_{Pt} = 57 μg cm^{-2}) and various thicknesses (Ω = 1600 rpm, ν = 5 mV s^{-1}). 0.1 M NaOH + 1 mM $NaBH_4$, 25 °C, argon atmosphere.

ough rinsing with ultrapure water (18.2 MΩ cm and <3 ppb total organic carbon (TOC), Millipore Elix + Gradient), as detailed in Ref. [32]. The cell was connected to a numeric potentiostat (Bio-Logic VMP2Z®) with a low-current option, controlled via EC-Lab® software (version 10.02, Bio-Logic®). An Hg-HgO (0.1 M NaOH) reference electrode was used (E = +0.165 V vs. SHE), as well as a gold mesh counter electrode and a gold sphere auxiliary electrode, the latter aiming at decreasing the experimental noise, as detailed in Ref. [56]. During each measurement, the cell was regulated at 25 ± 1 °C and permanently maintained under argon atmosphere (Messer 4N5) to eliminate traces of dissolved oxygen.

The procedure used to investigate the mass-transport effects during the BOR are based on linear and cyclic voltammetries, both in natural diffusion (Ω = 0) and diffusion-convection ($\Omega \neq 0$) regime. The potential sweep rate and the time spent at the initial potential (usually, the open-circuit potential) were also varied.

3. Results and discussion

3.1. Pt/C

Fig. 2 displays representative quasi-steady state BOR linear sweep voltammograms obtained for Pt/C active layers of different thicknesses in the range 0.38–3 μm. The reference voltammogram for a smooth Pt electrode is also shown for comparison.

As already pointed out by Molina Concha and Chatenet [27], the thickest active layer (3 μm) yields larger limiting current (Fig. 2). As the active layer was always completely covering the geometric surface of the glassy carbon tip, such change in limiting current can be associated to a change in the n_{e-} involved in the BOR (Eq. (4)). More specifically, a larger apparent BOR faradaic efficiency ($n_{e-} \approx 8$) is obtained for the 3 μm-thick active layer, as compared to $n_{e-} \approx 3$ for the thinnest active layer (0.38 μm) and $n_{e-} \approx 2$ for smooth Pt. Such increased n_{e-} with the active layer thickness can be explained as follows: thicker active layers can trap both the H_2 and BH_3OH^- species generated by heterogeneous hydrolysis (Eq. (2)) and/or the possible hydride-containing BOR intermediates. Their increased residence time favors the completion of their oxidation (Pt is active both for the oxidation of BH_3OH^- and H_2 [23,26,27]), thereby yielding higher faradaic efficiency.

Additionally, the BOR onset potential shifts negative for thicker active layers. This finding is in line with the fact that some hydrolysis products or BOR intermediates are prone to be oxidized at lower potential than BH_4^- [12]. BH_3OH^- is, as expected, a likely candidate, as experimentally demonstrated for gold electrodes by Nagle and Rohan [50,51] and more recently by Molina Concha and Chatenet for Pt electrodes [26]: the onset of BH_3OH^- oxidation is shifted negative compared to that of BH_4^- oxidation. In opposition, the generation of H_2, which is oxidized at higher potential than BH_4^- on Pt [26,27], cannot explain such negative shift of the reaction onset. This scenario (1-production of BH_3-containing intermediate species; 2-desorption from the Pt surface and 3-back-diffusion in solution) agrees with the recent ab initio calculations of Rostamikia and Janik regarding the BOR on Pt(1 1 1): the oxidative adsorption of BH_4^- into $BH_3^* + H^*$ (* stands for species at the electrode surface), followed by the desorption of BH_3 was predicted by their model [57]. As borane fast generates BH_3OH^- in alkaline solution, one understands that if these species are formed and trapped within the pores of a Pt-containing active layer, they can be fast oxidized on another Pt site, which agrees with the voltammograms of Fig. 2.

One would have noticed that in Fig. 2, the active layer thickness and Pt-loading are varying in the same direction: the thickest active layer is also the one with the highest Pt loading. It is therefore impossible from Fig. 2 to exclude any Pt-loading effect on the observed experimental trend. The experiments of Figs. 3 and 4 enable going beyond this uncertainty.

In Fig. 3, active layers based on Pt/C (10, 20 and 40 wt.%) were elaborated at constant Pt loading (m_{Pt} = 57 μg cm^{-2}), but decreas-

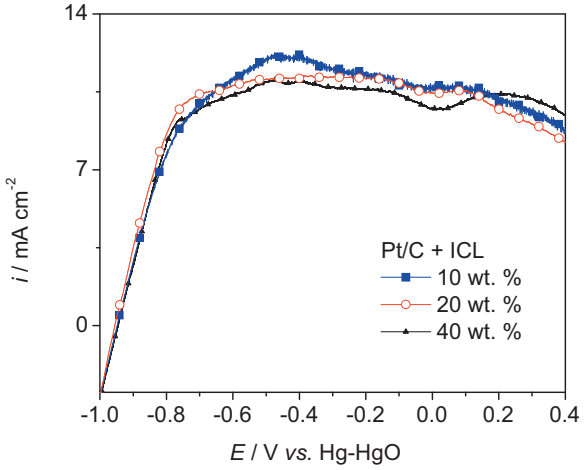

Fig. 4. $NaBH_4$ oxidation voltammograms plotted on Pt/C + Vulcan XC72 active layers of constant Pt-loading (m_{Pt} = 57 μg cm^{-2}) and constant thickness (3 μm); Ω = 1600 rpm, ν = 5 mV s^{-1}, 0.1 M NaOH + 1 mM $NaBH_4$, 25 °C, argon atmosphere.

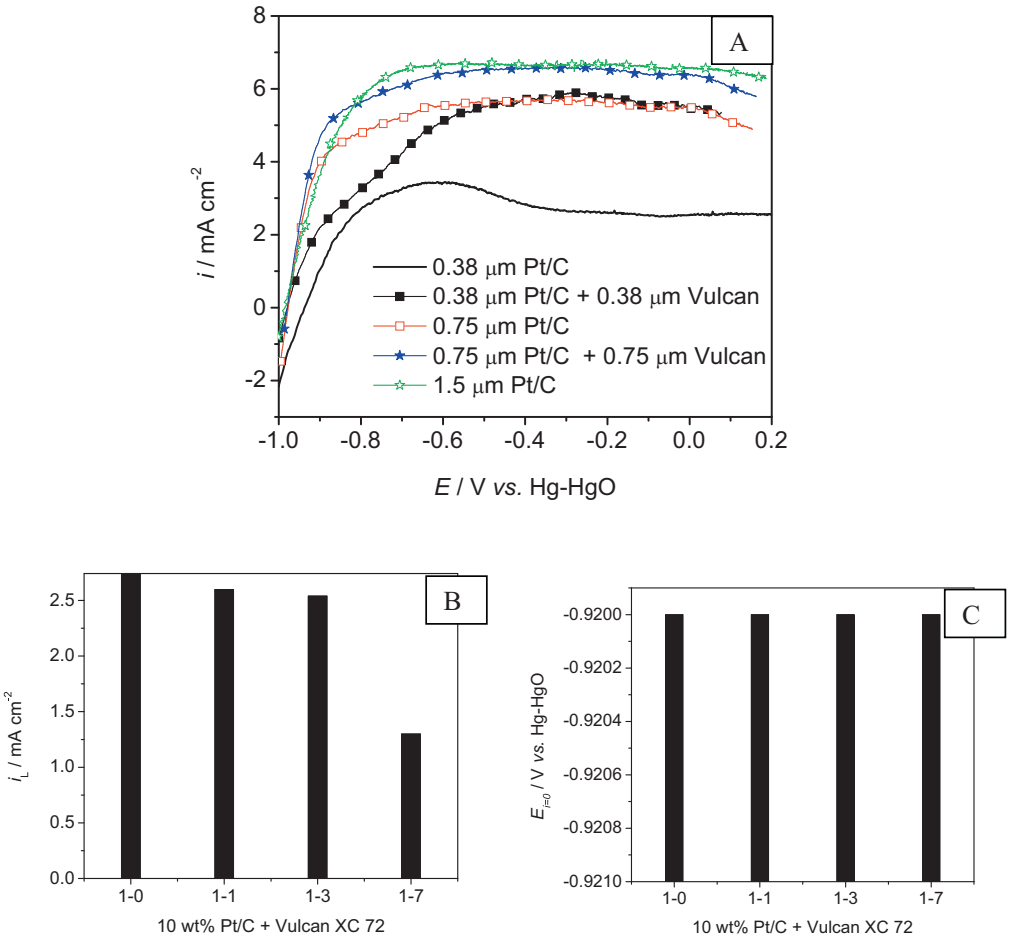

Fig. 5. (A) $NaBH_4$ oxidation voltammograms plotted on various 10 wt.% Pt/C + Vulcan XC72 active layers of various thickness and Pt loading, $\Omega = 900$ rpm, $\nu = 5\ mV\ s^{-1}$, $t_{ocp} = 10$ s. Variation of (B) the limiting current density and (C) the reaction onset ($E_{i=0}$) for BOR voltammograms recorded for active Pt/C layers of constant thickness (3 μm) and decreasing Pt loading: 10 wt.% Pt/C + ICL (1–0; 1–1; 1–3; 1–7) (same experimental conditions as in (A)).

ing thickness. Like for Fig. 2, Fig. 3 shows that the onset decreases and the limiting current density (faradaic efficiency) increases for thicker active layers, confirming the existence of an active layer thickness effect. However, the trend in Fig. 3 is not as pronounced as in Fig. 2, showing that a Pt-loading effect was also at stake in Fig. 2. The latter operates because the BOR is a slow reaction and "enough" Pt sites are required to quantitatively oxidize the BH_4^- species that reach the electrode. In addition, the results from Fig. 3 may be subjected to the well-known particle-size-effect that proceeds in electrocatalysis for many multiple-steps reactions [58]. Fig. 4 enables going beyond this uncertainty.

The data presented in Fig. 4 are relative to uniform active layers, consisting of a blend of catalytic material and inert carbon black (Vulcan XC72). For the 3 active layers considered, both the layer thickness (3 μm) and the platinum loading ($m_{Pt} = 57\ \mu g\ cm^{-2}$) were kept identical: 10 wt.% Pt/C, 20 wt.% Pt/C + Vulcan XC72 (1–1) and 40 wt.% Pt/C + Vulcan XC72 (1–3), so that only the size of the platinum particles varies.[2] Fig. 4 clearly exhibits the same faradaic efficiency and onset potential for all active layers of constant thickness and constant Pt loading, thereby demonstrating that the size-effect mentioned above is not determining for the BOR in the conditions investigated here.

Fig. 5A compares the BOR voltammograms obtained in diffusion-convection regime, for several couples of active layers of constant thickness and decreasing Pt-loading. For example, the Pt loading is kept constant (ca. 7 $\mu g_{Pt}\ cm^{-2}$) between the "0.38 μm Pt/C" trace and the "0.38 μm Pt/C + 0.38 μm Vulcan" trace, while the active layer thickness varies by a factor of 2 (0.38 vs. 0.75 μm). Comparing these two sets of data shows the strong effect of the active layer thickness on both the reaction onset and the limiting current: the thick active layer yields to a higher limiting current and slightly lower BOR onset potential. Alternatively, when one compares the results for actives layers of identical thickness but different Pt loading (e.g. comparing the "0.38 μm Pt/C + 0.38 μm Vulcan" and "0.75 μm Pt/C" traces or the "0.75 μm Pt/C + 0.75 μm Vulcan" and "1.5 μm Pt/C" traces), both the reaction onset (linked to the accumulation/oxidation of very oxidizable intermediates like BH_3OH^-) and limiting currents (linked to the complete oxidation (at least at sufficiently high potential) of BH_4^- and its oxidation/hydrolysis intermediates species, upon trapping within the active layer) remain unchanged. The voltammograms are however strongly varying with the Pt loading in the region of mixed kinetics/diffusion, which one may link to the slow kinetics of the BOR. In this region, the potential is too low to enable sufficiently fast oxidation of the BH_4^-/intermediate species present within the active layer, some of which therefore being prone to back-diffuse in solution without being oxidized.

Fig. 5B shows that sufficient Pt loading is necessary to promote complete oxidation of BH_4^- (even for thick active layers). In other

[2] The 10, 20 and 40 wt.% Pt/C electrocatalysts from E-Tek, display mean particle sizes of 2.3, 2.8 and 4.6 nm, respectively [59].

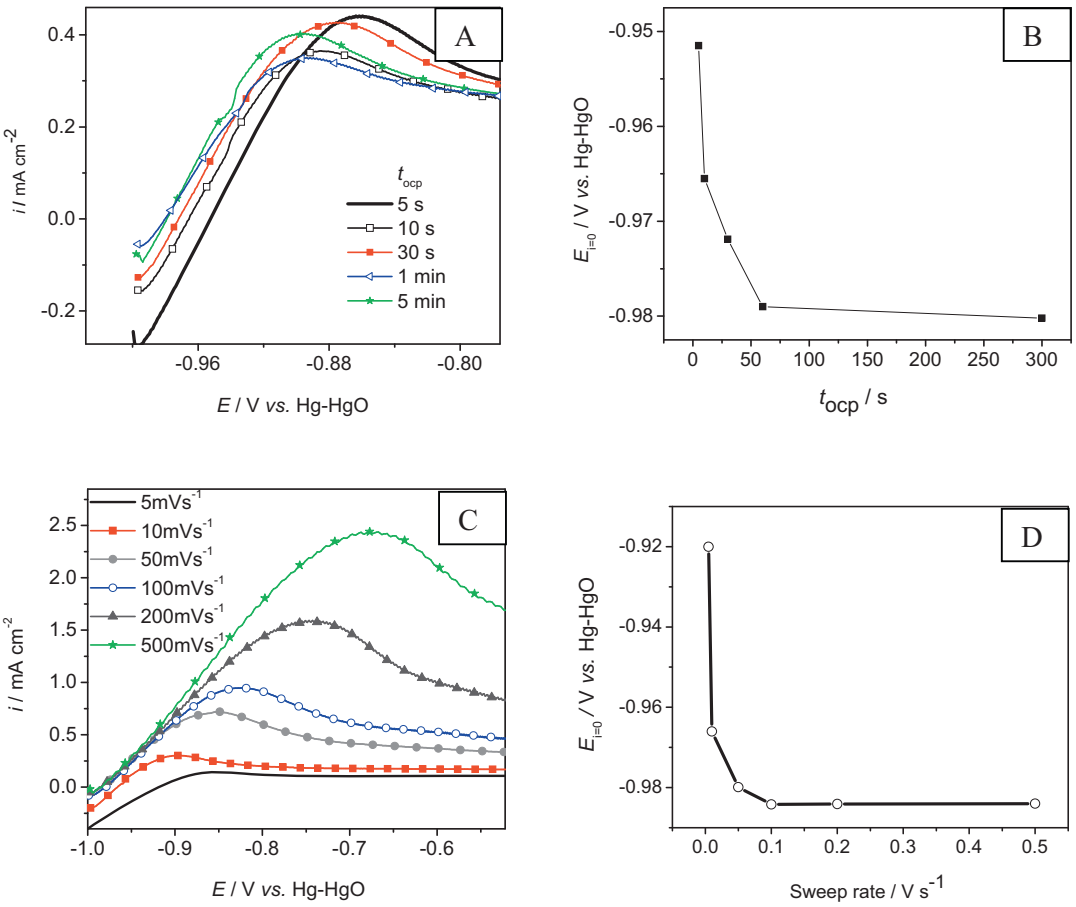

Fig. 6. (A) Anodic sweep of BOR cyclic voltammogram obtained on a smooth Pt electrode in 0.1 M NaOH + 1 mM $NaBH_4$ at $\nu = 20\,mV\,s^{-1}$, for various holding times at open circuit potential (t_{ocp}) and (B) corresponding variation of the reaction onset potential ($E_{i=0}$); (C) anodic sweep of BOR cyclic voltammogram obtained on a smooth Pt electrode in 0.1 M NaOH + 1 mM $NaBH_4$ at various scan rates ($t_{ocp} = 30\,s$) and (D) corresponding variation of the reaction onset potential ($E_{i=0}$). Argon atmosphere, $T = 25\,^{\circ}C$.

words, enough Pt sites are required to complete the reaction; when the Pt sites are too "diluted" in the active layer, some BOR intermediates can diffuse out without reacting. On the contrary, Fig. 5C, confirms that the reaction onset is constant for constant active layer thickness, because even when a little number of Pt sites are available, some extent of oxidation of BH_3OH^- can still proceed at low potential on the few Pt sites available.

To summarize, the results obtained in (Figs. 2–5) for Pt/C electrocatalysts do indicate that the apparent faradaic efficiency (n_{e-} involved in the BOR) and reaction onset potential both strongly depend on the thickness of the active layer of electrocatalysts, i.e. on the residence time of the reactant/intermediate species. Concerning the former effect, this is no surprise: it is somewhat classical that the completion of a multi-step reaction requires (i) sufficient catalyst loading (amount of catalytic sites) as well as (ii) sufficient residence time for the intermediates, as thoroughly discussed, e.g. in the case of the ORR [45–47]. Even though it is clear such effect are particularly at stake for 3D active layers, the next section will nevertheless address such issue for smooth platinum electrodes.

3.2. Pt

It is no secret that Pt promotes the heterogeneous hydrolysis of BH_4^- at open-circuit potential (see for example Refs. [23,26,40]). As the first step of the heterogeneous hydrolysis generates H_2 (oxidized above BH_4^- oxidation onset [26]) but also BH_3OH^- (oxidized at lower potential than BH_4^-), one may question whether the characterization procedure of the BOR on smooth Pt does influence the results obtained. To be more specific, do the potential sweep rate (ν) and time at ocp (t_{ocp}) before the anodic potential sweep of the voltammetry determine the reaction onset?

Fig. 6A shows linear sweep voltammograms obtained in natural diffusion condition for smooth Pt, when the measurements are performed at $\nu = 20\,mV\,s^{-1}$ for various initial holding times at the open-circuit potential before the voltammetric cycle: $t_{ocp} = 5$, 10, 30, 60 and 300 s. The beneficial influence of long-duration initial hold at the ocp is clear: the BOR apparent onset indeed shifts negative for increasing t_{ocp} (Fig. 6B). The rationale for that is the generation of BH_3OH^- at ocp that can somewhat "accumulate" at the interface prior its (fast) oxidation during the subsequent anodic scan.

In Fig. 6C the potential scan rate was varied in the sequence $\nu = 5$, 10, 20, 50, 100, 200, and $500\,mV\,s^{-1}$, while t_{ocp} was kept constant ($t_{ocp} = 30\,s$). In these conditions, the onset shifts negative for increasing scan rates (Fig. 6D). What happens is that BH_3OH^- species, which are spontaneously formed on Pt at ocp (in addition to H_2), do not have enough time to diffuse away from the electrode surface during the CV. They can therefore be oxidized in the anodic sweep for fast scan rates, whereas for slow scan rates, their back-diffusion into the solution becomes more important and detrimental to the BOR completion.

Fig. 6 confirms that the initial steps of the BOR (that determine the BOR onset potential) are strongly depending on the residence time of the heterogeneous hydrolysis/direct oxidation products, mostly because species being oxidized more easily than BH_4^- (like BH_3OH^-) are formed at the electrode surface. Obviously, one may wonder whether the existence of an inactive porous layer (the so-

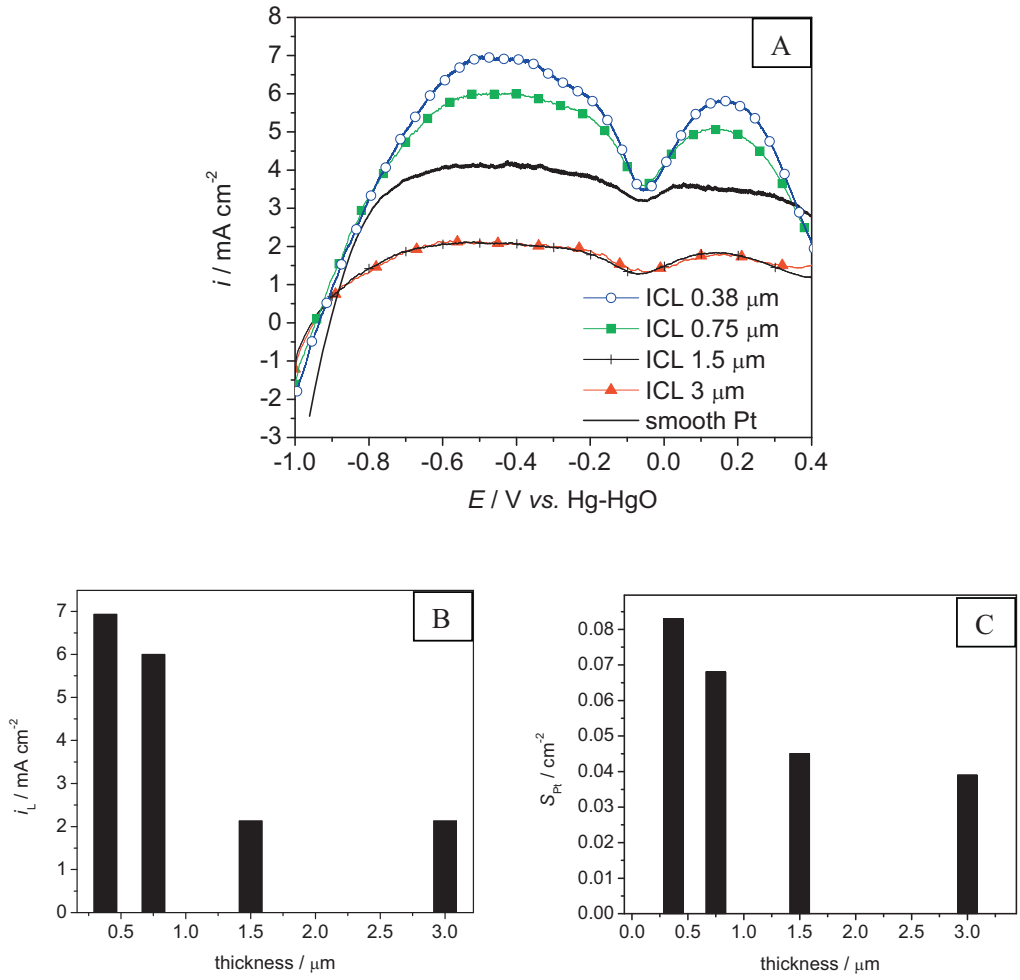

Fig. 7. (A) Anodic sweep of BOR cyclic voltammogram obtained on a smooth Pt electrode in 0.1 M NaOH + 1 mM $NaBH_4$ (t_{ocp} = 10 s, ν = 5 mV s^{-1} and Ω = 1600 rpm), for various thicknesses of inert carbon layers (ICL) deposited at the Pt surface. Argon atmosphere, T = 25 °C. Variation of (B) i_L and (C) the electrochemical active area of Pt (S_{Pt}, measured from hydrogen desorption coulometry, assuming 210 μC cm_{Pt}^{-2}) related to the voltammograms of (A).

called inert carbon layer, ICL, in the following) deposited at the smooth Pt electrode, that would enable BH_4^- species to reach the Pt surface but prevent the fast diffusion of the soluble products (e.g. BH_2 or BH_3 species [16]) generated at the electrode surface away from the surface, has a marked effect on both the BOR onset and apparent faradaic efficiency. To investigate this hypothesis, BOR voltammograms were plotted on smooth Pt electrodes covered with an inert Vulcan XC72 carbon layer (ICL) in diffusion-convection regime (Fig. 7). Two opposite trends are monitored on the reaction onset/limiting current (apparent faradaic efficiency):

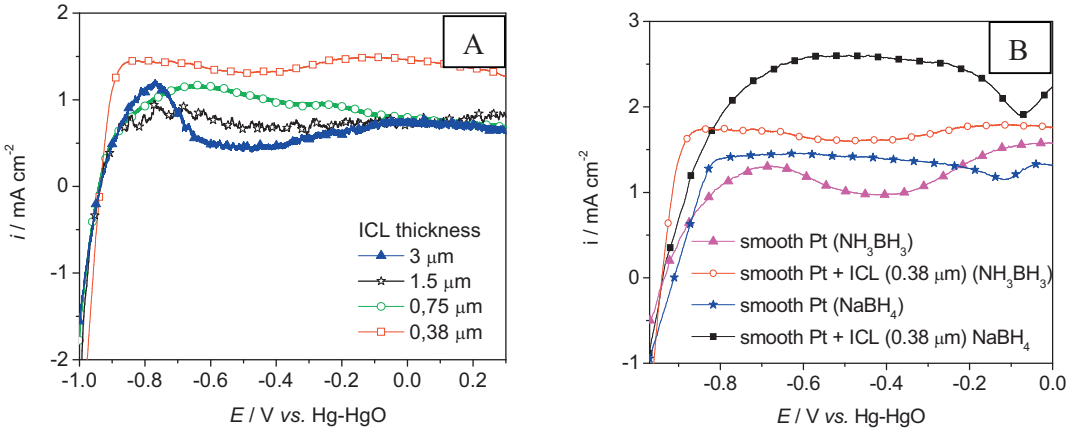

Fig. 8. (A) Anodic sweep of BOR cyclic voltammogram obtained on a smooth Pt electrode in 0.1 M NaOH + 1 mM NH_3BH_3 (t_{ocp} = 10 s, ν = 5 mV s^{-1} and Ω = 400 rpm), for various thicknesses of inert carbon layers (ICL) deposited at the Pt surface. (B) Comparison of the anodic sweep of BOR cyclic voltammogram obtained on a smooth Pt electrode + ICL (0.38 μm) in 0.1 M NaOH + 1 mM $NaBH_4$ or 0.1 M NaOH + 1 mM NH_3BH_3 (t_{ocp} = 10 s, ν = 5 mV s^{-1} and Ω = 400 rpm) and a smooth Pt electrode in 0.1 M NaOH + 1 mM $NaBH_4$ or in 0.1 M NaOH + 1 mM NH_3BH_3. Argon atmosphere, T = 25 °C.

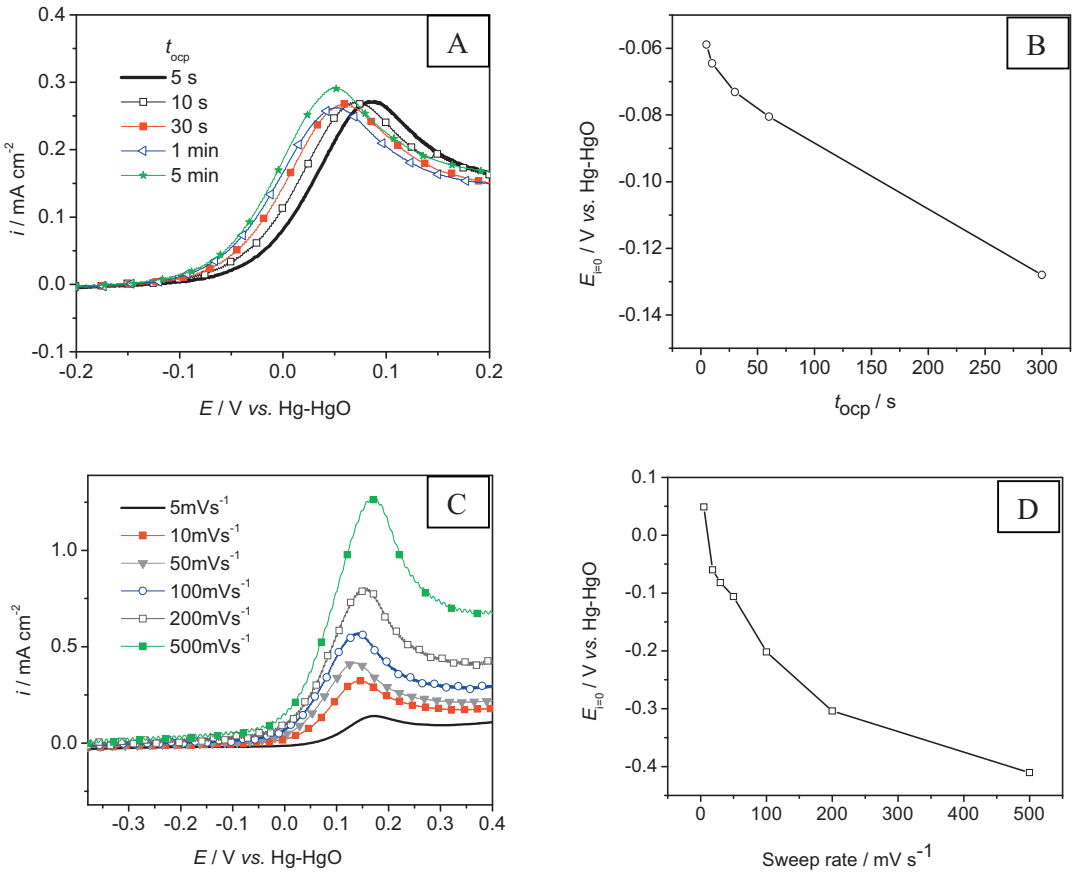

Fig. 9. (A) Anodic sweep of BOR cyclic voltammogram obtained on a smooth Au electrode in 0.1 M NaOH + 1 mM $NaBH_4$ at $\nu = 20\,mV\,s^{-1}$, for various holding times at open circuit potential (t_{ocp}) and (B) corresponding variation of the reaction onset potential ($E_{i=0}$); (C) anodic sweep of BOR cyclic voltammogram obtained on a smooth Au electrode in 0.1 M NaOH + 1 mM $NaBH_4$ at various scan rates ($t_{ocp} = 30\,s$); (D) corresponding variation of the reaction onset potential ($E_{i=0}$). Argon atmosphere, $T = 25\,°C$.

while the ICL covers some of the active surface, resulting in non-negligible decrease of the limiting current, because most of the geometric area of the smooth Pt is not accessed anymore, it also traps some direct oxidation/heterogeneous hydrolysis intermediates close to the place where they have been formed (i.e. at the vicinity of the Pt|ICL|electrolyte interface) and favors their (more) complete oxidation (at the Pt surface). This compromise results in the shape of the CV traces in Fig. 7A on the one hand the reaction onset shifts slightly negative with increasing thickness of the ICL (higher trapping ability of the ICL); on the other hand, the apparent faradaic efficiency is maximal for thin ICL (0.38 μm in the present case) (Fig. 7B). Indeed, thicker ICL mask most of the Pt surface (Fig. 7C) thereby preventing any quantitative reaction. It is also wise noting that, as expected, the faradaic efficiency reached for smooth Pt + ICL electrodes in no case equals that obtained for Pt/C active layers (compare the limiting current values of Figs. 3 and 4 for Pt/C vs. Fig. 7 for smooth Pt + ICL). As the BOR is overall slow, one indeed needs sufficient catalytic sites to perform it completely.

If NH_3BH_3 (a species that spontaneously yields BH_3OH^- in alkaline solutions [50]) is present in solution, the ICL has a negligible effect on the reaction onset (Fig. 8A), because BH_3OH^- is present in the bulk solution. On the contrary, when no ICL is present, the BH_3OH^- formed at the smooth Pt electrode are not trapped, resulting in a $NaBH_4$ oxidation onset shifted positive relative to (i) that in NH_3BH_3 solution for a smooth Pt electrode and (ii) that of $NaBH_4$ oxidation at Pt + ICL electrode (Fig. 8B). In the two last cases, BH_3OH^- are indeed present in the vicinity of the Pt surface, resulting in lower reaction onset potential. As a result, the reaction onset for a smooth Pt electrode in NH_3BH_3 is similar to that of (Pt + ICL) in $NaBH_4$. This set of data provides an indirect proof that BH_3OH^- is indeed formed on Pt at ocp and oxidized immediately above ocp, as discussed above and in [26,27].

3.3. Au and Au/C

The Sections 3.1 and 3.2 did put into evidence the non-negligible effect of the operating/mass-transport conditions on both the BOR

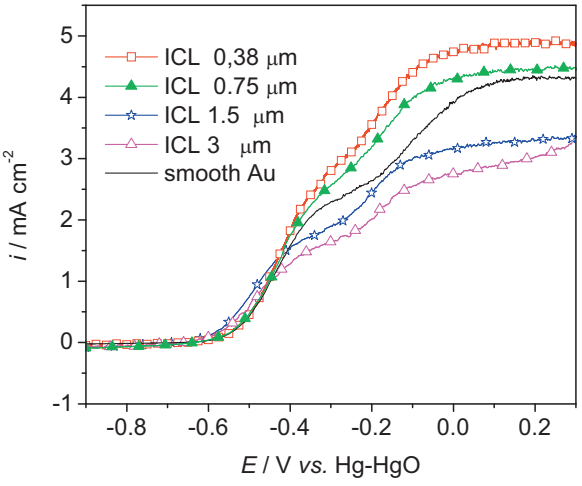

Fig. 10. Anodic sweep of BOR cyclic voltammogram obtained on a smooth Au electrode in 0.1 M NaOH + 1 mM $NaBH_4$ ($t_{ocp} = 10\,s$, $\nu = 5\,mV\,s^{-1}$ and $\Omega = 1600\,rpm$), for various thicknesses of inert carbon layers (ICL) deposited at the Au surface. Argon atmosphere, $T = 25\,°C$.

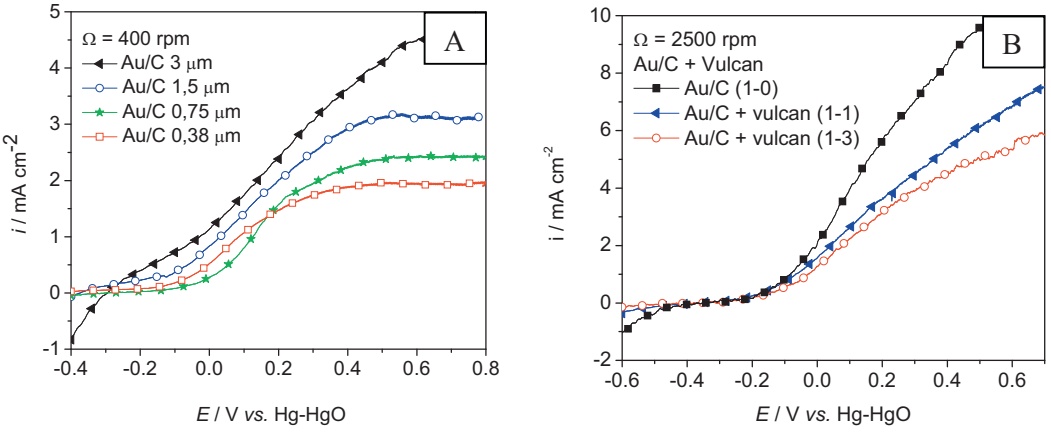

Fig. 11. $NaBH_4$ oxidation voltammograms plotted on (A) Au/C active layers of various thicknesses and Au loading (m_{Au} = 7, 14, 29 and 57 μg_{Au} cm^{-2} for the active layer thicknesses of 0.38, 0.75, 1.5 and 3 μm, respectively); Ω = 400 rpm, and (B) Au/C + Vulcan XC72 active layers of identical thickness (3 μm) and decreasing Au loading (m_{Au} = 14, 29 and 57 μg_{Au} cm^{-2} for the Au/C (1–0), Au/C + Vulcan (1–1) and Au/C + Vulcan (1–3) layers, respectively) – 0.1 M NaOH + 1 mM $NaBH_4$, 25 °C, argon atmosphere, $\nu = 5$ mV s^{-1}.

onset potential and apparent faradaic efficiency for Pt electrodes. The present section investigates whether such effect is at stake also for gold-based electrodes.

Fig. 9A shows linear sweep voltammograms obtained in natural diffusion condition for smooth Au (ν = 20 mV s^{-1}) with various initial holding times at the open-circuit potential: t_{ocp} = 5, 10, 30, 60 and 300 s. The beneficial influence of long-duration initial hold at the ocp is even clearer for Au than for Pt: the BOR onset shifts negative for increasing t_{ocp}, by several 10 mV (Fig. 9B).

When the potential scan rate was varied in the sequence ν = 5, 10, 20, 50, 100, 200, and 500 mV s^{-1} at constant t_{ocp} = 30 s, the onset also strongly shifts negative for increasing scan rates (Fig. 9C and D). This behavior is much larger than for smooth Pt (see Fig. 6), because the onset of BH_3OH^- oxidation is ca. 400 mV negative to that of BH_4^- on Au [50,51] (on Pt, the difference is only on the order of a few mV [23,26]).

Similarly to what was observed for smooth Pt covered by increasing thickness of inert carbon layers (ICL) (see Fig. 7), there exists an optimum of ICL thickness at which the interplay between the positive trapping effect of reaction intermediates and negative masking effect of the Au (active) surface (Fig. 10). However, conversely to what was observed for Pt, Au only yields to quantitative heterogeneous hydrolysis positive to the ocp (with the generation of H_2 [19,22] and BH_3OH^- [16–18]) and Au is rather inactive towards the oxidation of H_2. So, the effect observed here is only related to the oxidation of borohydride-containing intermediates of BH_4^- oxidation/hydrolysis (the possible H_2 produced being lost for any electron count).

Such trapping and subsequent oxidation of the BOR/hydrolysis intermediates is also observed when active layer of Au/C (10 wt.%) are considered (Fig. 11A), both in terms of onset potential and limiting current (apparent faradaic efficiency). Except for the inversion recorded between the 0.38 and 0.75 μm-thick active layers, the thicker the Au/C (10 wt%) active layer (and the Au loading), the more negative the onset potential and the larger the limiting current. Like in Fig. 2 regarding Pt/C (10 wt.%) active layers, one would note that the effects of the active layer thickness and Au loading are coupled in Fig. 11A.

Fig. 11B relative to Au/C + Vulcan XC72 active layers of identical thickness and decreasing Au loading, demonstrates the strong effect of the Au loading on the overall current. This was expected because the BOR kinetics on Au is by far inferior to that on Pt [23]. However, one remarks that when the active layer thickness is fixed, the reaction onset potential is fixed also.

4. Concluding remarks

The borohydride oxidation reaction (BOR) was studied on active layers composed of Vulcan XC72 carbon-supported Pt by voltammetry in 0.1 M NaOH/10^{-3} M $NaBH_4$. The n_{e-} value involved in the BOR was found to strongly depend on the thickness of the electrocatalyst active layer. Thin Pt/C active layers yield to incomplete BOR, while sufficiently thick layers (approximately 3 μm) yields to $n_{e-} \approx 8$, as a result of increased residence time of the BOR intermediates/heterogeneous hydrolysis products within the active layer. The onset of the BOR also depends on the presence of these reaction intermediates at the vicinity of the electrode surface, as demonstrated for smooth Pt electrode covered by inert carbon layers that act as trap for the reaction intermediates. Similar effects are observed for gold electrodes.

These results show that not only the nature of the metal electrocatalyst is of importance to reach high BOR efficiency, but also puts into evidence the role of the active layer structure/thickness on the BOR pathway/completion. In particular, the electrode processing (smooth surface vs. active layer of high-area catalysts, presence or not of a barrier for the back-diffusion of the reaction intermediates) as well as the operating conditions (time spent at ocp, revolution rate of the RDE, potential sweep rate) used to characterize the BOR all play an important role regarding the results obtained (in terms of overall faradaic efficiency and reaction onset). Knowing that the BOR is a very complex process, involving many chemical (hydrolysis) or electrochemical steps and yielding a large number of intermediates, this explains why the literature is often contradictory regarding apparently simple properties of BOR electrocatalysts, like the faradaic efficiency (number of electrons exchanged per BH_4^- species). In addition, only a limited number of studies have provided strong (physical) evidence about the nature of the intermediates at stake during the BOR, sometimes leaving a non-acceptable place for postulated BOR pathways/mechanism so far. While this is already very detrimental when smooth (simple) electrode surfaces are considered, this is even worse for the high surface-area (technological) electrocatalysts that will necessarily be used in DBFC electrodes. In conclusion, the characterization of such materials regarding the BOR (mandatory to enable the future development of commercial DBFC systems) should be done with tremendous care, because the intrinsic kinetic activity of these materials might be blurred/masked/modified by the existence of strong mass-transport effects at/within the active layer considered. Although the present paper did only investigate this issue for Pt and

Au-based surfaces/active layers, it is likely that it proceeds as well for any BOR catalysts.

Acknowledgements

The authors thank the CAPES/COFECUB (project Ph 598/08) and the "cluster énergie" of Région Rhône-Alpes (France) for funding.

Appendix A. Supplementary data

Supplementary data associated with this article can be found, in the online version, at doi:10.1016/j.cattod.2011.01.051.

References

[1] Z.P. Li, B.H. Liu, K. Arai, K. Asaba, S. Suda, J. Power Sources 126 (2004) 28.
[2] R.K. Raman, N.A. Choudhury, A.K. Shukla, Electrochem. Solid State Lett. 7 (2004) A488.
[3] Z.P. Li, B.H. Liu, K. Arai, S. Suda, J. Alloys Compd. 404–406 (2005) 648.
[4] J.B. Lakeman, A. Rose, K.D. Pointon, D.J. Browning, K.V. Lovell, S.C. Waring, J.A. Horsfall, J. Power Sources 162 (2006) 765.
[5] R. Jamard, A. Latour, J. Salomon, P. Capron, A. Martinent-Beaumont, J. Power Sources 176 (2008) 287.
[6] J.L. Wei, X.Y. Wang, S.Y. Yi, C.L. Dai, N. Li, Prog. Chem. 20 (2008) 1427.
[7] M. Chatenet, B. Molina Concha, G. Parrour, J.-P. Diard, F.H.B. Lima, E.A. Ticianelli, Potential and limitation of the Direct Borohydride Fuel Cell. Special emphasis on the Borohydride Oxidation Reaction (BOR) mechanism and kinetics on gold electrocatalysts, in: U.B. Demirci, P. Miele (Eds.), Boron Hydrides, High Potential Hydrogen Storage Materials, Nova Science, New York, in press, https://www.novapublishers.com/catalog/product_info.php?products_id=13010.
[8] S.C. Amendola, P. Onnerud, M.T. Kelly, P.J. Petillo, S.L. Sharp-Goldman, M. Binder, J. Power Sources 84 (1999) 130.
[9] M.M. Kreevoy, R.W. Jacobson, Ventron Alembic 15 (1979) 2.
[10] J.A. Gardiner, J.W. Collat, J. Am. Chem. Soc. 87 (1965) 1692.
[11] J.P. Elder, A.H. Hickling, Trans. Faraday Soc. 58 (1962) 1852.
[12] J.H. Morris, H.J. Gysling, D. Reed, Chem. Rev. 85 (1985) 51.
[13] R.L. Pecsok, J. Am. Chem. Soc. 75 (1953) 2862.
[14] M.E. Indig, R.N. Snyder, J. Electrochem. Soc. 109 (1962) 1104.
[15] Y. Okinaka, J. Electrochem. Soc. 120 (1973) 739.
[16] M.B. Molina Concha, M. Chatenet, F. Maillard, E.A. Ticianelli, F.H.B. Lima, d.R.B. Lima, Phys. Chem. Chem. Phys. 12 (2010) 11507.
[17] B. Molina Concha, M. Chatenet, C. Coutanceau, F. Hahn, Electrochem. Commun. 11 (2009) 223.
[18] P. Krishnan, T.-H. Yang, S.G. Advani, A.K. Prasad, J. Power Sources 182 (2008) 106.
[19] M. Chatenet, F.H.B. Lima, E.A. Ticianelli, J. Electrochem. Soc. 157 (2010) B697.
[20] D. Hua, Y. Hanxi, A. Xinping, C. Chuansin, Int. J. Hydrogen Energy 28 (2003) 1095.
[21] B.H. Liu, Z.P. Li, S. Suda, J. Electrochem. Soc. 150 (2003) A398.
[22] M. Chatenet, F.H. Lima, E.A. Ticianelli, ECS Trans. 25 (2010) 39.
[23] D.A. Finkelstein, N.D. Mota, J.L. Cohen, H.D. Abruña, J. Phys. Chem. C 113 (2009) 19700.
[24] M. Chatenet, M.B. Molina-Concha, N. El-Kissi, G. Parrour, J.-P. Diard, Electrochim. Acta 54 (2009) 4426.
[25] J.H. Kim, H.S. Kim, Y.M. Kang, M.S. Song, S. Rajendran, S.C. Han, D.H. Jung, J.Y. Lee, J. Electrochem. Soc. 151 (2004) A1039.
[26] B. Molina Concha, M. Chatenet, Electrochim. Acta 54 (2009) 6119.
[27] B. Molina Concha, M. Chatenet, Electrochim. Acta 54 (2009) 6130.
[28] H. Cheng, K. Scott, J. Appl. Electrochem. 36 (2006) 1361.
[29] B.H. Liu, Z.P. Li, K. Arai, S. Suda, Electrochim. Acta 50 (2005) 3719.
[30] H. Cheng, K. Scott, J. Power Sources 160 (2006) 407.
[31] H. Cheng, K. Scott, Electrochim. Acta 51 (2006) 3429.
[32] M. Chatenet, B. Molina-Concha, J.-P. Diard, Electrochim. Acta 54 (2009) 1687.
[33] M. Chatenet, F. Micoud, I. Roche, E. Chainet, Electrochim. Acta 51 (2006) 5459.
[34] G. Parrour, M. Chatenet, J.-P. Diard, Electrochim. Acta 55 (2010) 9113.
[35] D.M.F. Santos, C.A.C. Sequeira, J. Electrochem. Soc. 156 (2009) F67.
[36] P.I. Iotov, S.V. Kalcheva, A.M. Bond, Electrochim. Acta 54 (2009) 7236.
[37] E. Gyenge, M. Atwan, D. Northwood, J. Electrochem. Soc. 153 (2006) A150.
[38] J.I. Martins, M.C. Nunes, R. Koch, L. Martins, M. Bazzaoui, Electrochim. Acta 52 (2007) 6443.
[39] R. Tarozaitė, L. Tamašauskaitė Tamašiūnaitė, V. Jasulaitienė, J. Solid State Electrochem. 13 (2009) 721.
[40] E. Gyenge, Electrochim. Acta 49 (2004) 965.
[41] J.I. Martins, M.C. Nunes, J. Power Sources 175 (2008) 244.
[42] C. Wu, H. Zhang, B. Yi, Catal. Today 93–95 (2004) 477.
[43] M. Chatenet, M. Aurousseau, R. Durand, F. Andolfatto, J. Electrochem. Soc. 150 (2003) D47.
[44] M. Chatenet, L. Génies-Bultel, M. Aurousseau, R. Durand, F. Andolfatto, J. Appl. Electrochem. 32 (2002) 1131.
[45] A. Schneider, L. Colmenares, Y.E. Seidel, Z. Jusys, B. Wickman, B. Kasemo, R.J. Behm, Phys. Chem. Chem. Phys. 10 (2008) 1931.
[46] M. Inaba, H. Yamada, J. Tokunaga, A. Tasaka, Electrochem. Solid State Lett. 7 (2004) A474.
[47] P.S. Ruvinskiy, A. Bonnefont, M. Houllé, C. Pham-Huu, E.R. Savinova, Electrochim. Acta 55 (2010) 3245.
[48] Z. Jusys, J. Kaiser, R.J. Behm, Langmuir 19 (2003) 6759.
[49] K. Bergamaski, A.L.N. Pinheiro, E. Teixeira-Neto, F.C. Nart, J. Phys. Chem. B 110 (2006) 19271.
[50] L.C. Nagle, J.F. Rohan, J. Electrochem. Soc. 153 (2006) C773.
[51] L.C. Nagle, J.F. Rohan, Electrochem. Solid State Lett. 8 (2005) C77.
[52] F. Gloaguen, F. Andolfatto, R. Durand, P. Ozil, J. Appl. Electrochem. 24 (1994) 863.
[53] L. Genies, R. Faure, R. Durand, Electrochim. Acta 44 (1998) 1317.
[54] L. Genies, Y. Bultel, R. Faure, R. Durand, Electrochim. Acta 48 (2003) 3879.
[55] E. Guilminot, A. Corcella, M. Chatenet, F. Maillard, J. Electroanal. Chem. 599 (2007) 111.
[56] C.C. Herrmann, G.G. Perrault, A.A. Pilla, Anal. Chem. 40 (1968) 1173.
[57] G. Rostamikia, M.J. Janik, Electrochim. Acta 55 (2010) 1175–1183.
[58] F. Maillard, S. Pronkin, E.R. Savinova, Influence of size on the electrocatalytic activities of supported metal nanoparticles in fuel cells related reactions, in: W. Vielstich, H.A. Gasteiger, H. Yokokawa (Eds.), Handbook of Fuel Cells, vol. 5, John Wiley & Sons, Inc., New York, 2009, pp. 91–111.
[59] F. Maillard, M. Martin, F. Gloaguen, J.M. Léger, Electrochim. Acta 47 (2002) 3431.